3.4 HIGH RESOLUTION FORECASTS OF SEASONAL PRECIPITATION IN THE SOUTH-EASTERN MEDITERRANEAN: ANALOGUES DOWNSCALING OF GLOBAL FORECASTS

Dorita Rostkier-Edelstein[1,2,*], Pavel Kunin[3], Yubao Liu[2], Wanli Wu[2], Thomas Hopson[2], Amir Givati[4], Gael Descombes[2] and Ming Ge[2]

[1]Israel Institute for Biological Research, Ness-Ziona, Israel
[2]National Center for Atmospheric Research, Boulder, CO, USA
[3]Life Science Research Institute, Ness-Ziona, Israel
[4]Israel Hydrological Service, Jerusalem, Israel

1. INTRODUCTION

Planning the seasonal use of water resources in advance is one of the most important missions in the semi-arid Eastern Mediterranean (EM). The area is characterized by complex topography, land-uses and coast-lines that lead to steep spatial gradients in the observed seasonal precipitation (see e.g. Figs. 1 and 2).

Global seasonal forecasts, available freely on-line up to 6 months in advance, issued by European and American forecasting centers, e.g. NCEP, ECMWF and the UK Met Office provide partial and incomplete information about the expected precipitation amounts in this area due to their coarse spatial resolution of ~200 km grid-size (see e.g. Fig. 3). Accurate and useful forecasts require finer spatial resolution ~~(~~on the scale of a few kilometers~~)~~.

The present paper presents statistical downscaling methods to refine the global seasonal forecasts over Israel that can be operationally implemented in real time on an inexpensive computational infrastructure.

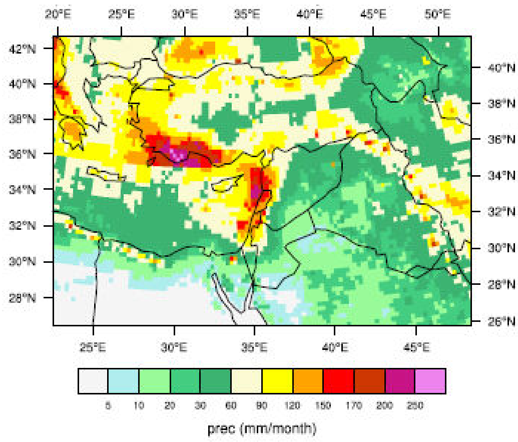

Fig. 1: Mean January precipitation for 2001–2006 over the area based data from the merged Tropical Rainfall Measurement Mission (TRMM) product (adapted from Hahmann et *al.* 2008)

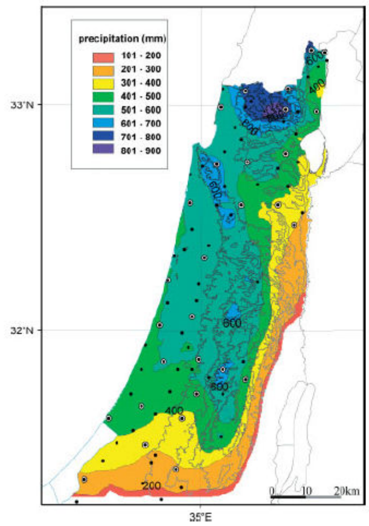

Fig. 2: 50-y average rainfall for the months November-March, based on 1954-2004. Black circles denote the 79 monthly long-record rainfall stations and the black circles encircle by white denote the 30 daily long-record rainfall stations. Height contours are in resolution of 200m and rainfall contours (isohyets) are in resolution of 100mm (adapted from Saaroni et *al.* 2010).

2. CHARACTERISTICS OF THE SEASONAL PRECIPITATION IN THE AREA

2.1. Physical factors

Hahmann, et *al*. (2010) and references therein have summarized the prevailing meteorological process responsible for the precipitation characteristics over Israel. We briefly summarize the main facts: Israel is located in the EM,

* *Corresponding author address:* Dorita Rostkier-Edelstein, Israel Institute for Biological Research, Environmental Sciences Division, Ness-Ziona, Israel; email: doritar@iibr.gov.il, rostkier@ucar.edu

a transition area between the subtropical high-pressure belt and the midlatitude westerlies. Superimposed on the large-scale processes are mesoscale effects related to the complex coastlines and terrain. The precipitation season extends from September to May and the most significant amounts are observed during the cold-season, i.e., December-January-February (DJF).

The precipitation is associated with Mediterranean cyclones whose climatology has been described in several works cited in Hahmann, et *al*. (2010). There are strong near-coastal gradients in observed precipitation, the positions of which have vast hydrologic consequences. These gradients are the result of the preferred cyclones tracks, their intensity and their interaction with the local topography. The spatial distribution of the precipitations varies from year to year due to the inter-annual variability of the frequency of the various types of cyclones.

Thus, proper estimation of the seasonal precipitation over this region requires correct simulation of the synoptic flow dominated by extra-tropical cyclones (proper seasonal frequency of cyclones) as well as the mesoscale flow dictated by the complex coast and terrain forcing.

2.2. Classification of weather regimes.

Alpert, et *al*. (2004) classified the daily synoptic-scale flow in the EM region into 19 weather regimes or classes using a semi-objective method. The classification of weather regimes is based upon the NCEP/NCAR Reanalysis Projerct (NNRP) dataset that extends from 1950 to the present and uses 25 of its grid points surrounding the EM coast at 2.5°×2.5° horizontal resolution as shown in Fig. 4. The classification procedure uses the geopotential height (Z), the temperature (T) and the U and V wind-vector components at the 1000 hPa pressure level to identify the various types of flow. A "reference" NNRP sub-set for the years 1985 and 1992 was subjectively classified by the authors into 19 weather classes. An analogue approach based on standardized minimum-Euclidean distances was used to classify the rest of the NNRP dataset with respect to the reference sub-set.

Saaroni, et *al.* (2010) have shown that the intensity and spatial distribution of the precipitations during the wet season is correlated to the different cyclones types in Alpert et *al*. (2004), as classified according to their depth and location. Moreover, the variability from season to season is a result of the rate of occurrence of the various types of cyclones that varies from season to season.

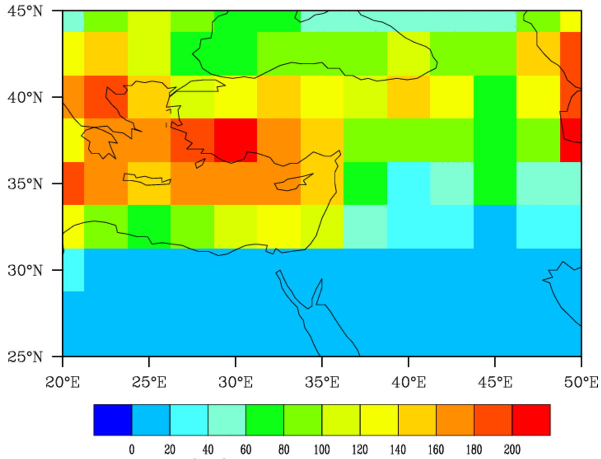

Fig. 3: A typical CFS1.0-ensemble mean precipitation-rate forecast map zoomed into the EM (this specific forecast was issued on October 2009 and shows a forecast for January 2010).

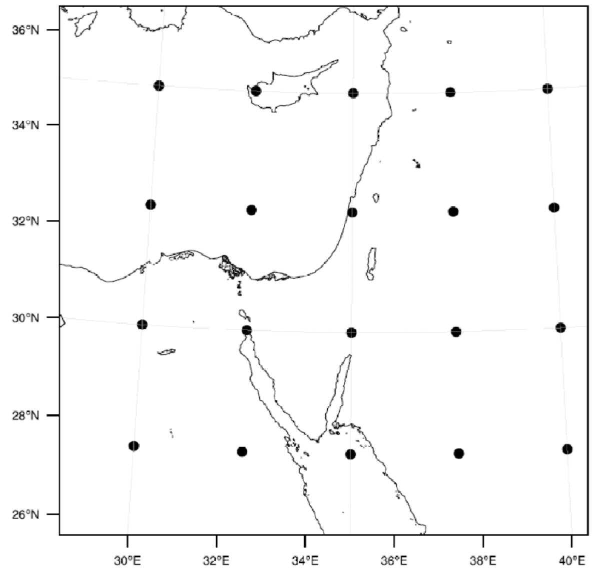

Fig. 4: The 25 grid points used in the weather-regimes classification procedure of Alpert *et al.*, 2004.

3. STATISTICAL DOWNSCALING ALGORITHMS

Statistical downscaling is based upon statistical links between large(r)-scale weather and observed local-scale weather. It is computationally inexpensive and suitable for our purposes as we are interested in an operational tool that can be run on a desktop/laptop computer.

Our algorithms are based on the relationship between the large-scale flow associated with the EM cyclones and the spatial distribution of precipitation at pre-determined gauge stations.

3.1. Gauge stations

After performing a thorough analysis of a gauges precipitation database we selected a sub-set of 18 reliable stations within the chosen main hydrological basins (out of a database of hundreds of stations). These selected stations provide a continuous long-term archive of daily precipitations and have undergone a trustable quality assurance procedure. We stress the need for a reliable long-term precipitation record in order to develop a precise statistical downscaling algorithm. Fig. 5 displays the location of the 18 stations on the regional map.

3.2. Weather-Regimes Downscaling (WRD)

Motivated by the works of Alpert, et *al*. (2004) and Saaroni, et *al*. (2010), we have developed a weather-regimes analogue-type statistical-downscaling algorithm based on the correlation between the frequency of the 19 weather classes and the local precipitation. We refer to this method as WRD.

First, for the selected stations we calculate the monthly multi-year-mean precipitation associated with each of the weather regimes using the archived observed precipitation and the NNRP dataset (that has been classified into weather regimes using standardized minimum-Euclidean distances with respect to the reference NNRP sub-set). The synoptic-scale flow of the seasonal-global forecasts may be classified into the 19 weather regimes by calculating their standardized minimum-Euclidean distances with respect to the NNRP classified dataset. The frequencies of each weather regime in the seasonal-global forecasts are then calculated and used to predict the future local precipitation by weight-averaging the multi-year mean precipitation amounts corresponding to the various weather regimes with those frequencies. The method may be considered an analogues-matching algorithm, in which the closest analogue is used to determine the weather class.

Since we can only find similar but not identical weather conditions in the past, the use of weather categories and mean precipitation amounts per category is used to introduce an estimate of the uncertainty in our forecast. We also stress the importance of using the 25 grid points individually, rather than considering spatial-averaged values, a strategy that could simplify our algorithm. Similar spatial-averaged values may lead to very different locations of the lows minima and gradients resulting in very different spatial precipitation distributions. In other words, spatial averaging over the 25 grid points makes the large-scale information even coarser. Fig. 6 presents a flow chart of the algorithm.

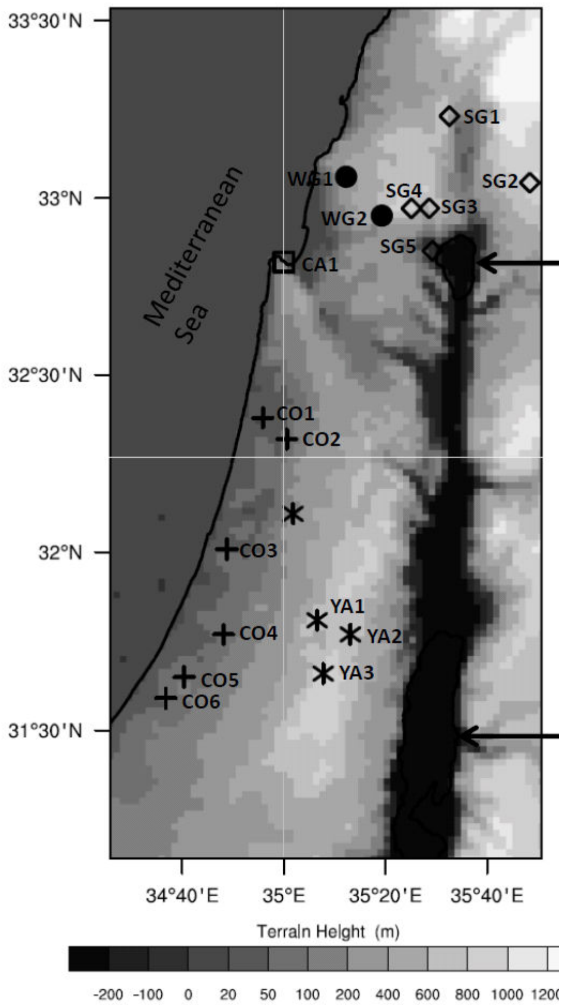

Fig. 5: The location of the 18 selected stations on top of the topography. Different symbols and naming are used for the different basins: Coastal (+, CO), Carmel (□, CA), Western Galilee (●, WG), Sea of Galilee/Kinneret (◊, SG), Mountain/Yartan (*, YA).

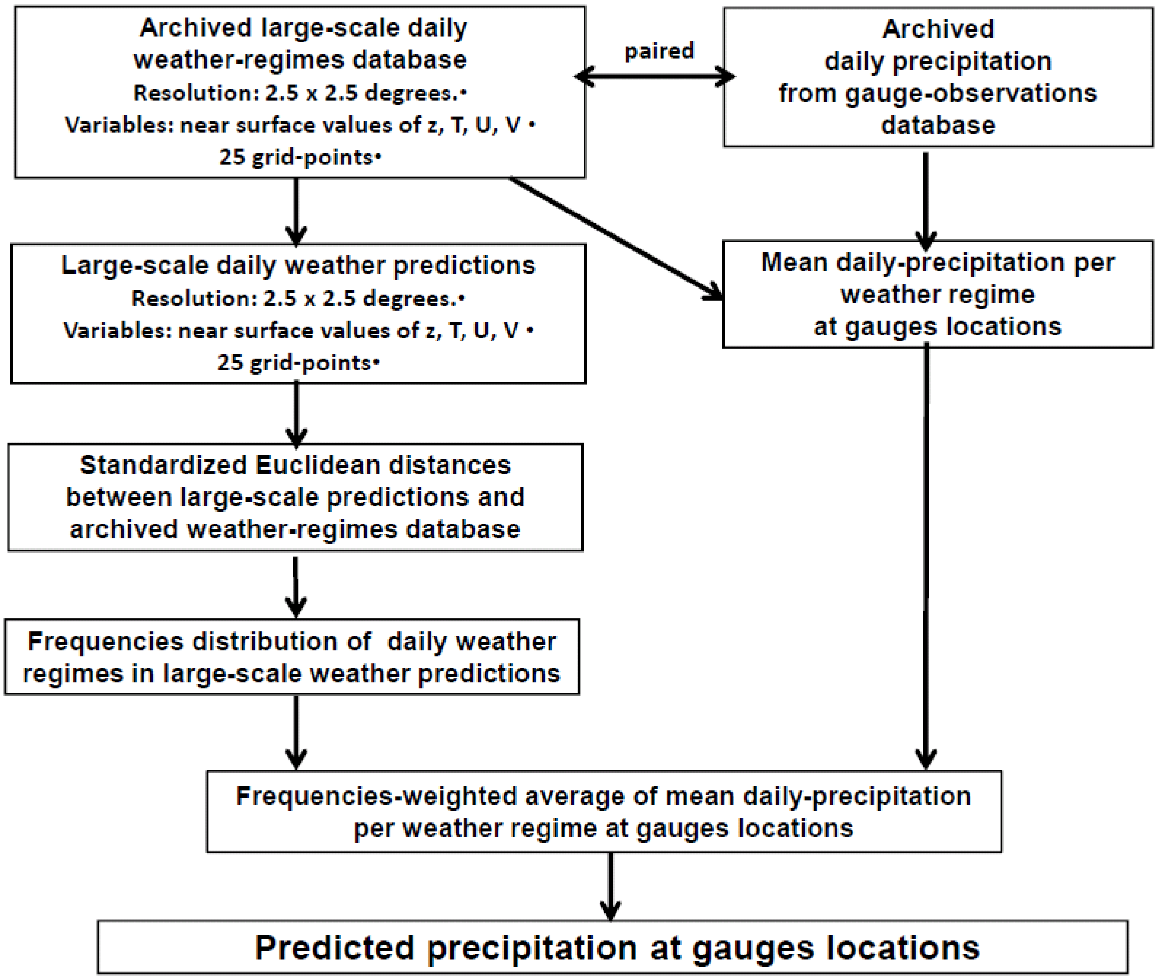

Fig. 6: Flowchart of the weather-regimes downscaling (WRD) algorithm using Alpert et *al.* (2004) 19 weather classes.

3.3. Analogues Downscaling (AN)

Our second strategy relies on a simple analogues technique using the same large-scale variables and grid-points as chosen by Alpert, et *al*. (2004), but without considering the classes defined in that work. We find the past analogues closest to the future event according to the standardized-Euclidean distances and weight the daily precipitation in inverse proportion to their squared distances. By doing so, we take into account small differences in the large-scale weather patterns that were neglected in the classification into a small number of categories as defined by Alpert, et *al.* (2004). The use of more than one analogue (we considered up to 6 closest analogues) introduces the uncertainty due to the fact that only approximate analogues may be found. Monthly precipitation is simply the sum of the daily amounts. Fig. 7 presents a flow chart of the algorithm.

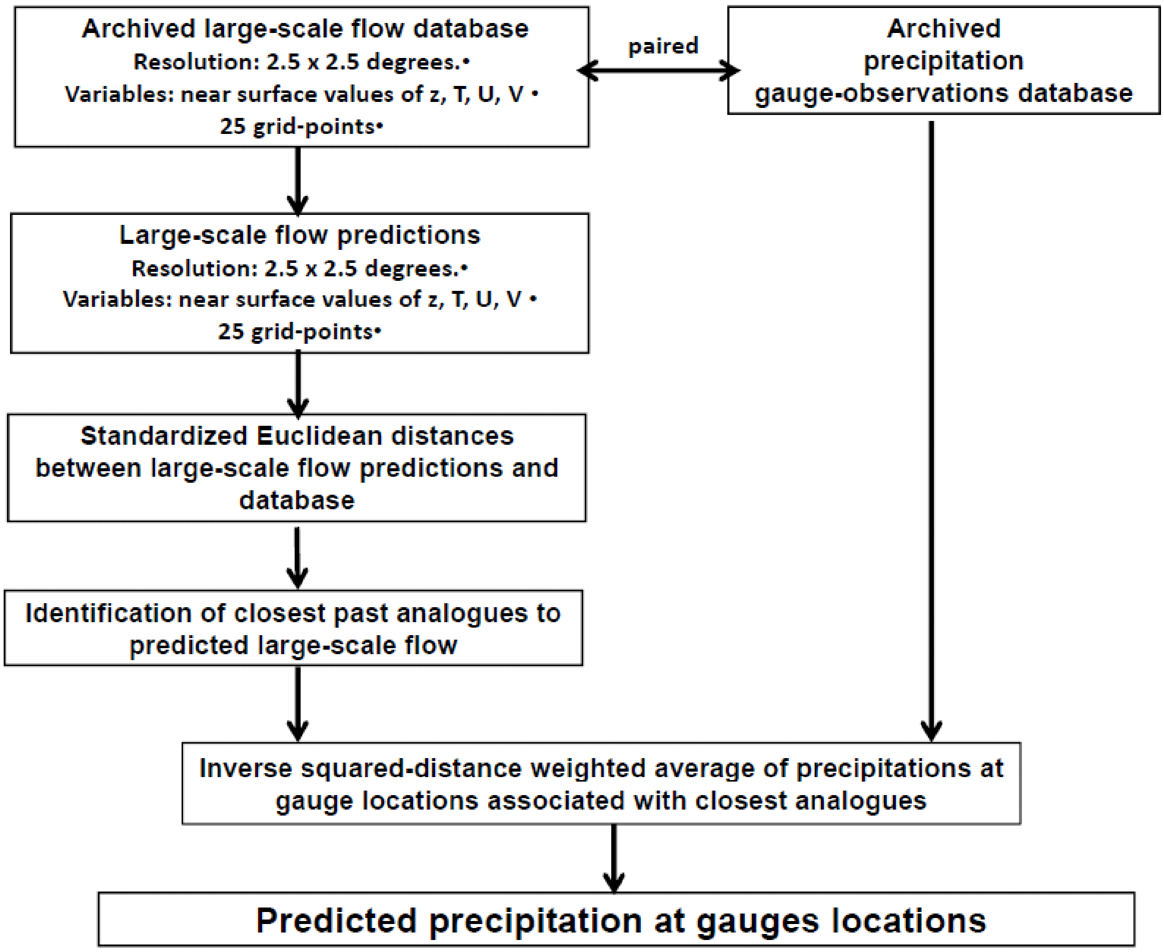

Fig. 7: Flowchart of the analogues downscaling (AN) algorithm.

4. VALIDATION USING NNRP

4.1. Rationale

Prior to being used to downscale real-seasonal forecasts, the algorithm was validated using the accurate large-scale circulation patterns provided by the NNRP dataset. In doing so, we assume "perfect large-scale flow" and test the accuracy of the other components of the algorithm. It should be noted that the large-scale flow simulated by the global-seasonal forecasts is expected to be less accurate than that reproduced by reanalysis as these are run in a hindcast mode (for periods of time in the past) including assimilation of meteorological observations which mitigate model errors, whereas observations are obviously not available for forecasts estimating the flow at future times.

Our validation strategy consists of downscaling 21-27 wet seasons (between 1981 and 2008, depending on the availability of rain gauge observations) of the NNRP database. 18 wet seasons are used as a reference set for the weather regimes and analogues identification, and their corresponding precipitation at each station (1991-2008); the downscaled year is excluded from the reference set each time.

4.2. Validation results

The validation was designed to provide skill information that is useful to water resources managers.

4.2.1. Spatial and inter-annual variability

Figure 8 presents observed and NNRP-downscaled DJF precipitation, and the observed mean (we refer to this quantity as "climatological mean", calculated over the studied period), at each station, for two extreme seasons. The stations are ordered according to basins following the naming in Fig. 5. WRD predictions use up to two nearest weather regimes i.e. WRD2, AN predictions use up to three nearest analogues i.e. AN3. The use of additional past weather regimes/analogues within each of the methods does not lead to improvement.

The 1998-1999 season in Fig. 8a, depicts the driest season during the studied period and is characterized by large observed gradients among some stations located at different basins (as large as ~350 mm). At all stations, the observed precipitation was below its climatological mean. This pattern has been accurately reproduced by both downscaling methods. Both downscaling methods predict particularly well the inter-station gradients. The predictions by both methods are very similar, but the AN3 shows small advantage in 14 stations. The WRD2 method tends to slightly overestimate the observed precipitation amounts, in particular at the Carmel, Coastal and Yartan basins. These are the driest basins. The overestimation by the WRD2 method is a result of using the weather-regimes mean daily-precipitation as an estimate of the daily predicted precipitation, which may be a poor estimate of the lower extremes of the precipitation distributions associated with each regime. On the other hand, the use of single analogues, as is the AN3 method, introduces precise precipitation amounts of past extreme events.

The 2002-2003 season, Fig.8b, illustrates one of the wettest seasons in the studied period and is characterized by relatively large observed gradients among stations too (as large as 220 mm). Both prediction methods reproduce the inter-station variability to a significant extent. However, they both tend to underestimate the observed amounts to some level, in particular for stations showing extremely high amounts. In those cases, the AN3 outperforms the WRD2 predictions. The underestimation of extreme amounts results from the fact that only 3 wet seasons are observed in the historical set (excluding 2002-2003), illustrating the need for historical records as long as possible in statistical downscaling methods. The larger underestimation obtained in the WRD2 method is a result of using the weather-regimes mean daily-precipitation amounts as an estimate of the predicted daily precipitation, that poorly represent the upper extremes of the daily precipitation distributions associated with each regime. This is due to the fact that the daily precipitation distribution is skewed towards low values (not shown here). On the other hand, the use of single analogues, as is the AN3 method, introduces precise precipitation amounts of past extreme events.

4.2.2. Linear relationship between downscaled and observed seasonal precipitation

Figures 9a and 9b shows scatter plots of observed vs. NNRP-downscaled DJF precipitation using the WRD2 and AN3 methods, respectively, at the 18 selected stations for each of the seasons within the period 1981-2008. The full line represents the linear regression relationship between the observed and estimated values. The dashed line represents the $y=x$ line, i.e., the linear regression for a perfect model. Both figures show that the observed-precipitation distribution is skewed towards lower values with fewer events of DJF precipitation above 800 mm. Both methods show fair linear agreement between downscaled and observed precipitation. However, the WRD2 tends to underestimate the upper tail of the distribution and overestimate the low tail of it, for the reasons detailed in Section 4.2.1. Both methods explain about 80% of the observed variance, with little advantage in the AN3 method.

5. DOWNSCALING OF CFS1.0 ENSEMBLE OF SEASONAL FORECASTS

The CFS1.0-ensemble seasonal forecasts (Saha et *al.* 2006) were used to implement the AN3 algorithm in a real-time automatic operational mode. We have used all CFS1.0-ensemble members issued for a given month with initial conditions at the 1st through the 29th of each month. For each day four different members are issued. This provides a total of 116 members in our downscaled forecasts of each month. All of them are equally weighted.

The AN3 algorithm was applied to each of the CFS1.0-ensemble members, thus providing an ensemble of downscaled precipitation. Figure 10 compares the CFS1.0-downscaled (using the AN3 algorithm) DJF forecasts to the observed precipitation at each of the stations for the 2009-2010 and 2010-2011 seasons (CFS1.0 ensemble initial conditions issued in October). Downscaled-ensemble mean values are dressed with error bars that represent the ensemble spread.

In order to assess the accuracy of our algorithm during these seasons under the assumption of "perfect large-scale flow" we have also downscaled the corresponding NNRP set, results are presented in Fig. 11. The regression line shows good agreement between the observed and the NNRP-downscaled precipitation, and the R^2 value shows that the calculations account for 75% of the variance.

The linear regression for the CFS1.0-downscaled precipitation (Fig. 10) shows good agreement between observed and estimated values, very similar to that obtained when using NNRP as large-scale input (Fig. 11). The regression explains 67% of the variance, somewhat lower than that explained when using NNRP. The error bars show that the ensemble spread is a function of the mean-precipitation amounts; with larger uncertainty found for the larger mean values.

(a)

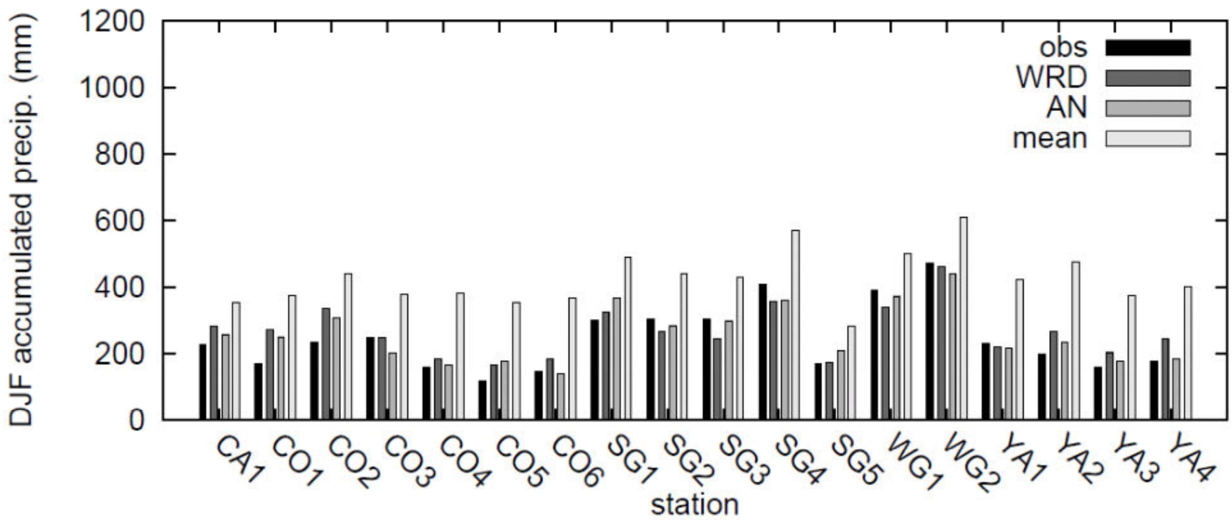

(b)

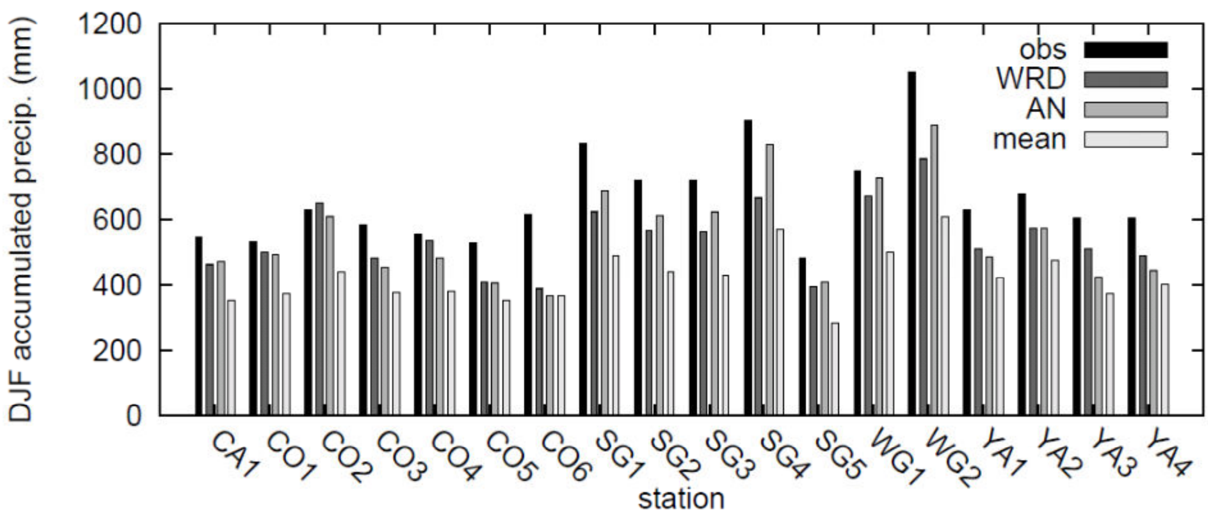

Fig.8: Observed, predicted, and climatological mean DFJ-precipitation at each station for (a) the driest among the studied seasons, (b) the wettest among the studied seasons. Stations are identified following the naming in Fig. 5. WRD predictions use up to two nearest weather regimes i.e. WRD2, AN predictions use up to three nearest analogues i.e. AN3.

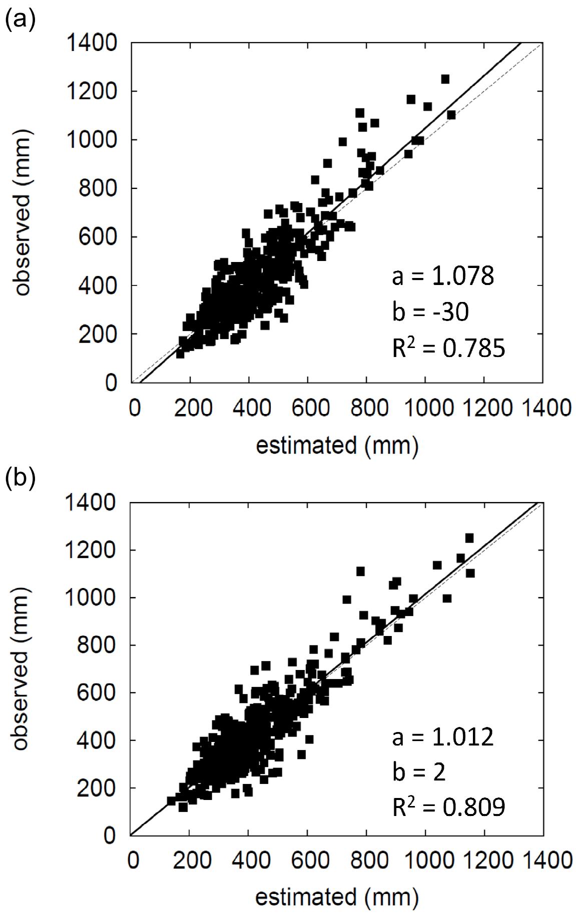

Fig. 9: Observed vs. NNRP-dowscaled DJF precipitation at the 18 selected stations for the seasons within the period 1981-2008. The full line represents the linear regression relationship between the observed and and estimated values. The dashed line represents the y=x line, i.e., the linear regression for a perfect model. (a) WRD2 method. (b) AN3 method.

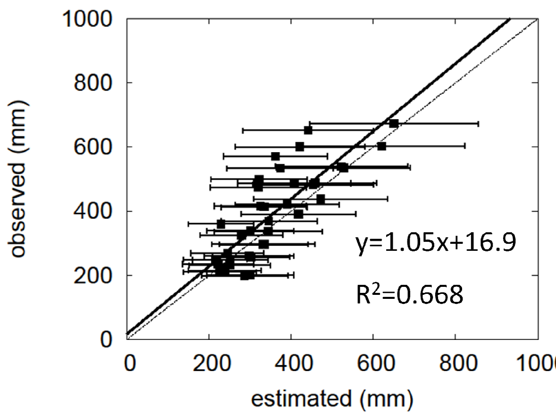

Fig. 10: Observed vs. CFS1.0-dowscaled (AN3 method) DJF precipitation at the 18 selected stations for the seasons 2009-2010 and 2010-2011 (CFS1.0 was initialized in October 2009 and 2010, respectively).

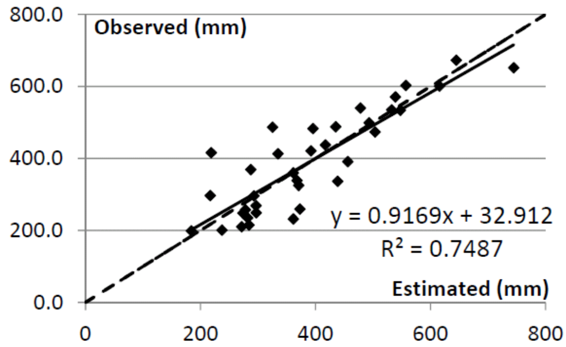

Fig 11: Observed vs. NNRP-downscaled (using the AN3 method) DJF precipitation at the 18 selected stations for the seasons 2009-2010 and 2010-2011.

6. SUMMARY

We presented two statistical downscaling methods to estimate precipitation at pre-determined stations. The methods are based on identifying daily large-scale past analogues of near-surface maps of winds, temperature and geopotential height (defined on 25-points grid at a 2.5° × 2.5° resolution) and correlating them with the past daily local precipitation. Two approaches were developed: one of them makes use of a classification of the large-scale weather patterns into regimes (WRD) and the other one is based on finding closest analogues without grouping the weather events into defined regimes (a "pure analogues" approach, AN).

The methods were validated at 18 reliable (long-term records) stations using accurate large-scale input provided by the NCEP/NCAR reanalyses. Our validation results proved good deterministic skill of the algorithms as measured by the linear correlation between predicted and observed precipitation amounts**.** The predicted results reproduce the observed inter-annual and spatial variability. The AN method was shown to provide more accurate estimations in reproducing extreme dry or wet seasons, as the use of the mean of the precipitation distribution associated with each weather-regime represents a poor representation of the distributions when these are skewed.

After validation the method was used to downscale 2 seasons of the operational CFS1.0-ensemble seasonal forecasts. When used with an ensemble of large-scale forecasts our method provides ensemble estimation as well. The mean-ensemble estimations at 18 stations were verified against observations. The verification shows good agreement between the observed and estimated precipitation for these two seasons. The spread of the ensemble is shown to encompass the observations, confirming the consistency of the ensemble results. The ensemble provides probabilistic information that can be useful to decision making.

Further improvement of the algorithm is possible by refining the weather-regimes classification or the identification of past analogues. This may be accomplished in several ways. First, a classification of weather regimes associated with precipitation would benefit from inclusion of physical variables at levels beyond the surface, for instance values of vorticity at upper levels. The inclusion of additional large-scale variables is expected to increase the variance explained by the method. Second, the determination of closest past analogues could be improved by including cross correlations between variables as is done in the calculation of Mahalanobis distances. Estimations of the precipitation associated with weather-regimes and of its uncertainty could be improved by re-sampling events within the specific classes.

The new updated CFS2.0 system is intended to provide more accurate large-scale forecasts and we expect the skill of the downscaled products to improve when CFS2.0 is used, too.

7. REFERENCES

Alpert P., I. Osetinsky, B. Ziv, & H. Shafir, 2004: Semi-objective classification for daily synoptic systems: Application to the eastern Mediterranean climate change, *Int. J. Climatol.,* **24**, 8, 1001-11

Hahmann, A.N., Rostkier-Edelstein, D., Warner, T.T., Liu, Y., Vandenberghe, F., Swerdlin, S.P., 2008: Toward a climate downscaling for the Eastern Mediterranean at high-resolution. *Adv. Geosci.*, **12**, 159–164. www.adv-geosci.net/12/159/2008/

Hahmann, A.N., Rostkier-Edelstein, D., Warner, T.T., Vandenberghe, F., Liu, Y., Babarsky, R., Swerdlin, S.P., 2010: A reanalysis system for the generation of mesoscale climatographies. *J. Appl. Meteor. Climatol*, **49**, 954–972, 10.1175/2009JAMC2351.1.

Saaroni H., N. Halfon, B. Ziv, P. Alpert and H. Kutiel, 2010: Links between the rainfall regime in Israel and location and intensity of Cyprus lows, *Int. J. Climatol*. DOI: 10.1002/joc.1912

Saha S., S. Nadiga, C. Thiaw, J. Wang, W. Wang, Q. Zhang, H. M. van den Dool, H.-L. Pan, S. Moorthi, D. Behringer, D. Stokes, M. Pena, S. Lord, G. White, W. Ebisuzaki, P. Peng, P. Xie, 2006: The NCEP Climate Forecast System. *J. Climate*, **19**, 3483-3517.